

## Research Article

# A Bioreactor Model of Mouse Tumor Progression

George A. Thouas, John Sheridan, and Kerry Hourigan

*Division of Biological Engineering, Faculty of Engineering, Monash University, Wellington Road, Clayton, Victoria 3800, Australia*

Correspondence should be addressed to George A. Thouas, george.thouas@eng.monash.edu.au

Received 17 December 2006; Revised 11 May 2007; Accepted 18 June 2007

Recommended by Abdelali Haoudi

The present study represents an investigation of a novel stirred bioreactor for culture of a transformed cell line under defined hydrodynamic conditions *in vitro*. Cell colonies of the EL-4 mouse lymphoma cell line grown for the first time in a rotating disc bioreactor (RDB), were observed to undergo changes in phenotype in comparison to standard, static flask cultures. RDB cultures, with or without agitation, promoted the formation of adherent EL-4 cell plaques that merged to form contiguous tumor-like masses in longer-term cultures, unlike the unattached spheroid aggregates of flask cultures. Plaques grown under agitated conditions were further altered in morphology and distribution in direct response to fluid mechanical stimuli. Plaque colonies grown in RDBs with or without agitation also exhibited significant increases in production of interleukin-4 (IL-4) and lactate, suggesting an inducible “Warburg effect.” Increases in cell biomass in RDB cultures were no different to flask cultures, though a trend toward a marginal increase was observed at specific rotational speeds. The RDB may therefore be a suitable alternative method to study mechanisms of tumor progression and invasiveness *in vitro*, under more complex physicochemical conditions that may approximate natural tissue environments.

Copyright © 2007 George A. Thouas et al. This is an open access article distributed under the Creative Commons Attribution License, which permits unrestricted use, distribution, and reproduction in any medium, provided the original work is properly cited.

## 1. INTRODUCTION

*In vitro* models of tumor biology are useful to better understand the biological processes that underlie neoplasia, such as tumor invasiveness [1] and angiogenesis [2]. These approaches utilize standard culture vessels (e.g., flasks, Petri dishes, or well plates) which are essentially variable sized, flat-bottomed plastic containers of millilitre capacity. For *in vitro* assays such as these, standard culture vessels are often modified by inclusion of adhesive monolayers and gel-like substrates [3]. Another important physical characteristic that is not normally included *in vitro* during tissue culture is hydrodynamics, which occurs naturally in living tissues. Hydrodynamic regimes are common operational features of many bioreactor and perfusion flow systems, both experimentally and commercially. A recent trend has been the widespread modification of these systems for tissue culture applications with incorporation of physiological characteristics (e.g., mimetic oxygenation and nutrient mass transfer characteristics) with prolonged culture sustainability, and for scalability of high-throughput processes such as in phar-

maceutical production [4]. The efficacy testing of bioreactor designs for mammalian tissue culture applications has often involved the use of transformed cell lines [5–8], due to their robustness and uniformity of growth for quantitative analysis. In relation to cancer biology, bioreactors have also shown further utility in the development of antineoplastic therapeutic strategies [9, 10].

Tissue culture bioreactors may also be useful for the elucidation of tumor cell progression under defined physicochemical conditions, such as under variable oxygen tensions and cell densities [11]. The potential improvements in the homogeneity of bioreactor cell populations for this purpose, as observed previously in comparison to standard vessels [12], may also be valuable for obtaining more reliable metabolic information about neoplastic phenotypes, with relevance to renewed interest in aberrant biochemical biomarkers of neoplasia for ongoing improvement of diagnostics and therapeutics [13, 14]. In the present study, a novel rotating disc bioreactor (RDB) was investigated for its efficacy in propagating a cancer cell line, with a view to develop a biomimetic model of tumor progression. Basic

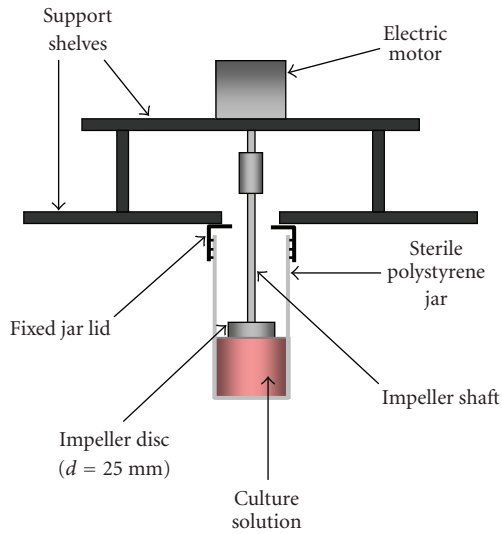


FIGURE 1: Schematic of the rotating disc bioreactor. Diagrammatic representation of the prototype rotating disc bioreactor rig designed for mammalian cell culture.

phenotypic features of mouse lymphoma (EL-4) cells [15], grown in suspension within stirred RDB vessels, were assessed in comparison to unstirred and standard static cultures in the present study.

## 2. METHODS

### 2.1. Bioreactor construction and modification for cell culture

The RDB rig was constructed as a support for an array of motorized disc impellers in vertical alignment with fixed, presterilized polystyrene jars (75-9922-412, Sarstedt, Numbrecht, Germany) (Figure 1). The entire rig was designed to be mounted within the tissue culture incubator (Figure 2) with a view to future modification as a stand-alone unit. The double-shelved platforms were constructed from hard-anodized aluminium, with six variable speed stepper motors (SD17, Sanyo-Denki, Tokyo, Japan) fixed to the upper shelf. Each motor supported machined solid metal impellers (diameter = 25 mm, thickness = 10 mm, surgical/pharmaceutical grade 316 stainless steel) in axial alignment with the jars. Motors were connected individually by cable to a digital-to-analog motion controller (PXI, National Instruments, Austin TX, USA) situated outside the incubator. The RDB rig and impellers were washed in a nonpyrogenic detergent, rinsed with filtered water and autoclaved before installation.

Calculation of the rotational speed of the motors was based on the inertia-to-viscosity ratio (Reynolds number,  $Re$ ) pertaining to axial fluid flow in a cylinder [16], defined by the equation

$$Re = \frac{\Omega r^2}{\nu}, \quad (1)$$

where  $r$  represents the disc radius (0.025 m),  $\nu$  represents the kinematic viscosity of the culture solution ( $1.592 \times 10^{-6} \text{ kgm}^{-1}\text{s}^{-1}$  at  $37^\circ\text{C}$ ) measured using a Couette viscometer (RFS II Rheometrics, Piscataway, NJ, USA), and  $\Omega$  represents the angular velocity of the disc ( $\text{rad}\cdot\text{s}^{-1}$  or  $60/2\pi$  rpm). A volume of 50 ml contained in the RDB vessels used in this study was used to give fluid aspect ratio of height/radius  $\approx 2$ . Previous observations using fluid mechanics models have demonstrated a well-blended [17] and well-oxygenated [18] laminar flow using similar fluid aspect ratios in a stirred cylinder. Use of a disc impeller situated at the fluid surface rather than at the cylinder base was chosen in this study to avoid leakage problems previously observed for the latter design [16] and potential contamination and biochemical degradation problems that may result from any form of leakage.

### 2.2. Computational modeling of bioreactor fluid flow patterns

Preliminary numerical simulations of fluid flow within RDBs, with dimensions of jars and impellers as outlined in the previous section, were performed using custom encoded fluid dynamics simulation software based on published methods [19]. Previous simulations of stirred cylindrical vessels have demonstrated an axisymmetric laminar vortex that recirculates, so that flow along the rotating base moves radially out toward the vessel wall [17, 20] and inward toward the axis near the fluid surface. In confirmation of those studies, a similar laminar flow pattern was simulated for the RDB, a surface disc, with more elongated streamlines at higher mixing rates, indicating more efficient recirculation of fluid from the lid to the vessel base (Figure 3) and implying potentially more efficient oxygenation. The use of a smaller diameter disc is also considered to be potentially less inhibitory to oxygen diffusion than those of diameters closer to the vessel diameter. For the present experiment, a range of rotational speeds of 0.7–70 rpm ( $Re = 10\text{--}1000$ ) were arbitrarily tested for their effects on cell growth. Lower  $Re$  values of the order of 10–100 are in accordance with values tested in other suspension bioreactors [6, 18]. Values of  $Re$  of 100–1000 represent previously untested values for a cell culture RDBs that correspond to efficient fluid mixing and subsequent oxygenation, though with the addition of potentially more damaging average shear stresses above  $Re = 600$  (Figure 4).

### 2.3. Preparation of cell cultures

EL-4 lymphoma cells were chosen for their robustness in culture, their growth as suspended aggregates, their utility for hybridomas for previous bioreactor studies [15, 21, 22], and for their sensitivity to mechanical stimuli [23]. EL-4 cells have also not previously been grown in bioreactor cultures. Frozen stocks of EL-4 cells were thawed and prepared for culture according to a generic immunology laboratory protocol [24], with the exception of the use of advanced minimal essential medium (Cat. no., 2492-013; Invitrogen,

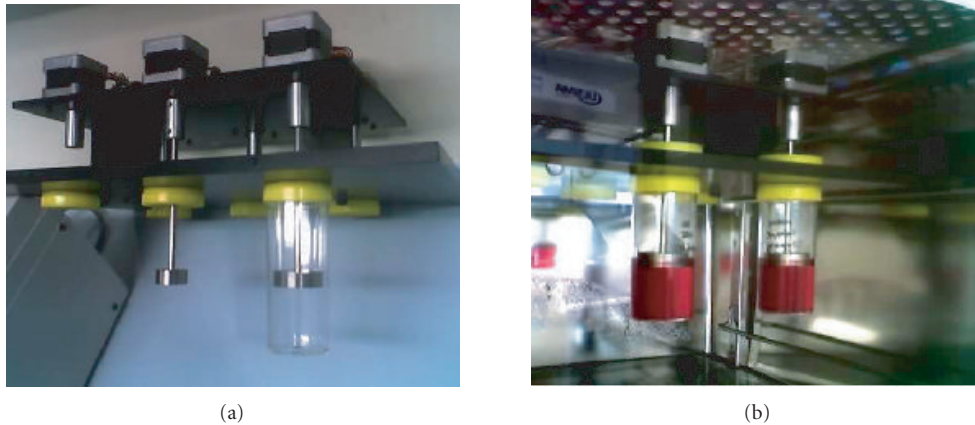


FIGURE 2: Photographs of the rotating disc bioreactor. (a) The bioreactor array prior to installation into a cell culture incubator. (b) Installed bioreactor with fixed vessels containing culture solutions with seeded EL-4 cells.

Carlsbad, Calif, USA) supplemented with 10% fetal calf serum ((FBS), Cat. no.10099-133, Invitrogen) as the culture solution. Thawed aspirates were centrifuged (500 g, 5 min, 4°C) and resuspended in this medium before seeding at a density of 10–20,000 cell/ml in 5 ml aliquots culture solution, allocated to 6-well tissue culture plates (Falcon 353046, BD) pre-equilibrated in a tissue culture incubator (BB15, Heraeus GmbH, Hanau, Germany, 37°C, humidified atmosphere 5% CO<sub>2</sub> in air). Seeded cultures underwent post-thaw recovery for 1–2 weeks before exponential population expansion. Established cultures were then maintained in this growth phase by twice-weekly subculture in tissue culture flasks.

For culture in RDB vessels, postexpansion EL-4 spheroids were resuspended in fresh, pre-equilibrated culture solution at a density of 10–15,000 cells/ml. Aliquots of 50 ml were then allocated from this pool to individual RDB vessels (test groups) or tissue culture flasks (control group). Bioreactor vessels were secured to the bottom shelf of the RDB rig with the impeller disc partially submerged and in continuous rotation throughout the culture period.

#### 2.4. Assessments of cell growth and morphology

Cell populations in tissue culture flasks and RDB vessels were quantitated by a packed cell volume (PCV) method designed for suspension bioreactors, using pre-calibrated PCV centrifuge tubes (TPP, Trasadingen, Switzerland) as described previously [25]. A calibration curve of cell density versus PCV was prepared with serially diluted aliquots of an expanded EL-4 culture of known density as determined by haemocytometer counts. The curve of best fit for this calibration was found to be  $y = 2.5652x^3 - 25.022x^2 + 102.35x + 0.3642$  ( $R^2 = 1$ ;  $x = \text{PCV tube capillary level } (\mu\text{m})$ ;  $y = \text{cell density } (x10^3 \text{ cells/ml})$ ). For RDB cultures, samples were removed after manual agitation to obtain a turbid solution with a visible absence of adherent colonies at the plastic base (the relatively loose substrate adhesion of EL-4 aggregates has been described previously [26], and in the present study negated the need for scraping or enzymatic digestion). Du-

plicate 1 ml samples of RDB suspensions were removed and assessed for PCV at the completion of culture, converted to cell density using the standard curve. Differences between seeded and postculture values of cell density were divided by the number of culture days and expressed as ratios of daily biomass increase. Gross morphology of EL-4 cell colonies grown in RDB vessels and flask cultures was observed with a dissection microscope. Images were captured using a digital CCD camera mounted on the microscope in conjunction with image acquisition software (ArcSoft, Fremont Calif, USA). Values of colony dimensions were quantitated manually from the same image data using the image processing software (Scion Image, Scion Corp, Frederick, Md, USA).

#### 2.5. Metabolic assays

Metabolic assessments of culture solution were assayed as a biochemical indicator of cell growth in response to altered physicochemical conditions, as described previously [27, 28]. The concentrations of glucose and lactate were measured simultaneously for individual medium supernatants taken from RDB vessel and flask cultures after centrifugation of cells. Assays were performed using proprietary enzyme-based colorimetric assay kits in conjunction with an automated ultraviolet/visible spectrophotometer system (Synchron LX, Beckman Coulter, Fullerton, Calif, USA). Millimolar concentrations of glucose and lactate measured in spent culture solutions were compared to values measured in samples of unseeded culture solutions. Daily lactate production was compared to daily glucose consumption as a ratio, which was then corrected for daily increase in biomass.

#### 2.6. Cytokine assays

Single-cell production of the cytokine interleukin-4 (IL-4) was measured using a proprietary enzyme-linked immunosorbent spot (ELISPOT) assay kit (Autoimmune Diagnostics, Strassberg, Germany). Expression of the same cytokine by EL-4 cells has been described previously [21],

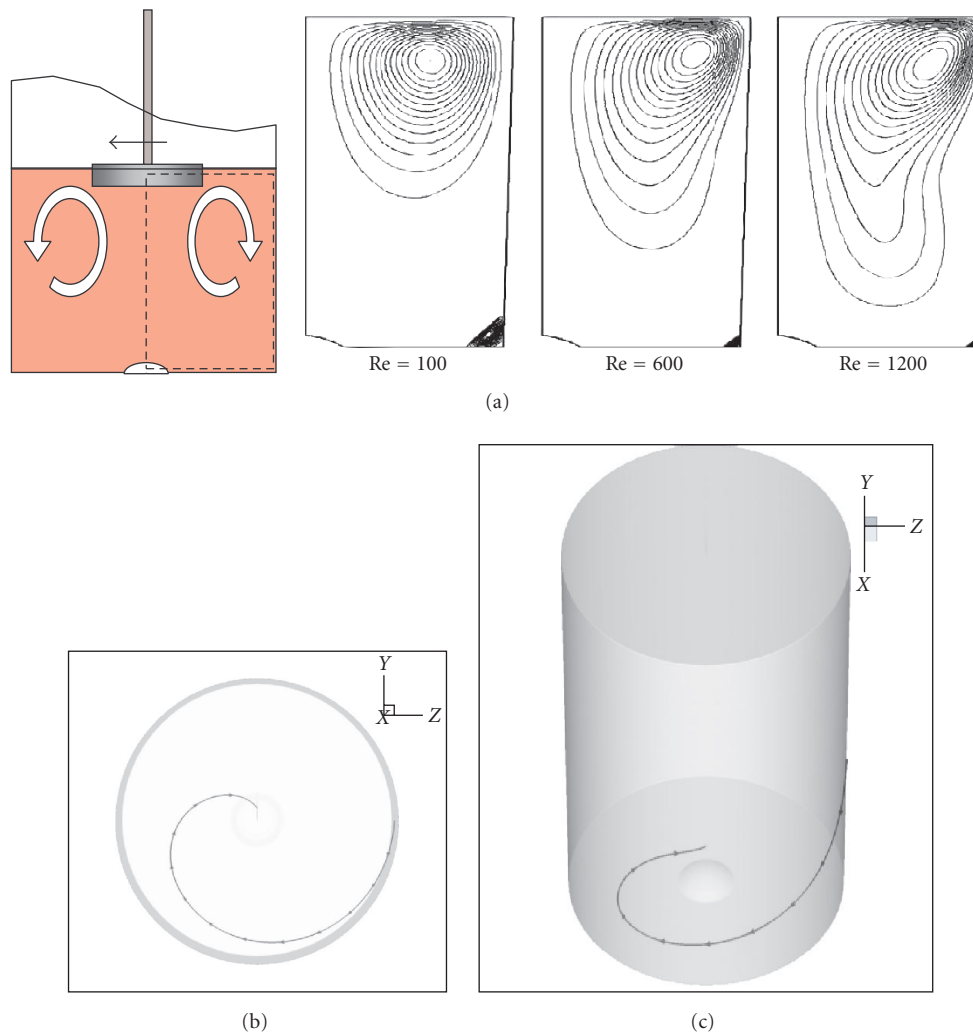


FIGURE 3: *Computational modeling of fluid flow patterns in the RDB.* (a) Cross sectional streamlines emanating from fluid surface in the vicinity of the fluid surface, demonstrating a laminar flow vortex pattern. (b) Simulated trajectory of a single semibuoyant particle (an idealized cell aggregate) moving passively in response to flow in the meridional direction. (c) Three-dimensional simulation of the same particle from (b) after having been seeded near the fluid surface, and coming to rest passively near the RDB vessel centre.

with differential expression in hybridoma cells produced in bioreactors under variable shear rates [27]. Samples of between  $10^6$  and  $10^7$  cells isolated from RDB vessel and standard cultures were incubated at decreasing dilutions overnight in multi-well plates precoated with anti-mouse monoclonal antibodies to adhesive polymer membranes. The secreted IL-4 captured on membranes was then incubated with biotinylated secondary antibodies after cell removal and reacted with a chromagen substrate to monochromatic spots. Individual wells were analyzed spectrophotometrically and assigned arbitrary spot forming units (SFU), in comparison to internal positive control cells (splenocytes) and in response to the control antigen concanavalin A.

## 2.7. Statistical analysis

Mean values of cell biomass increase and ELISPOT SFU values were log-transformed (log function) and compared us-

ing Tukey's ANOVA. The normality of biomass increase ratios in stirred and unstirred bioreactors was tested using the Kolmogorov-Smirnov test. Ratios of lactate and IL-4 production between RDB vessels and flasks were log-transformed and compared using an unpaired  $t$  test. Only differences between means with a  $p$ -value of 0.05 or less were included, and considered biologically significant.

## 3. RESULTS AND DISCUSSION

### 3.1. Morphological observations of EL-4 bioreactor cultures

After seeding, EL-4 cell colonies grown in RDB vessels settled randomly to the vessel base within hours, and remained there for the duration of culture. At the completion of culture, RDB vessels (without agitation) were observed to contain irregularly shaped, adherent plaques dispersed evenly

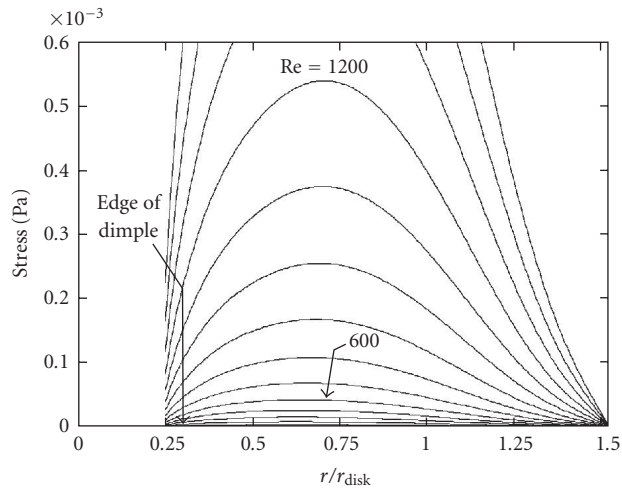


FIGURE 4: Relationship between fluid shear stress and location at the RDB vessel base. Computational simulation of shear stresses calculated at the vessel base with respect to distance away from centre axis, expressed as the ratio of base radius ( $r$ ) to the impeller disc radius ( $r_{\text{disk}}$ ) (Pa = pascal). The term “dimple” represents the small dome-shaped manufacturing artefact observed in the centre all RDB disposable vessels, representing a nonideal boundary.

across the vessel base (approx. 40 plaques/cm<sup>2</sup>) (Figure 5(a)). Circumferentially, these plaques were flattened and densely packed, whereas centrally the plaques had merged to form a contiguous confluent layer. In the intervening area of the vessel base, plaques presented as discrete adhesions with asymmetric boundaries, in either a focal punctate form (approx. of 200  $\mu\text{m}$  in diameter) or a flattened discoid form (approx. 500  $\mu\text{m}$  in diameter).

Compared to RDB vessels cultured without agitation, cultures that had been agitated contained larger discoid plaques (approx. 800  $\mu\text{m}$  diameter) that were fewer in number (approx. 7 plaques/cm<sup>2</sup>) and located predominantly near the vessel circumference (Figure 5(b)). In addition, these plaques were generally circular and discoid with smooth edges, and with approximately half of the plaques exhibiting a more oval shape with the longer axis aligned with the axial flow direction. A centrally located discoid tumor-like mass of confluent cells was also observed in stirred RDB vessels, which could be maintained for several weeks (Figure 5(c)). While flask control cultures also exhibited some partially adherent colonies, a majority of the colonies were irregularly shaped, suspended spheroids (approx. 50–200  $\mu\text{m}$ ) that were macroscopically visible in solution (Figures 5(d), 5(e)).

Variable rates of impeller stirring of RDB vessels resulted in a trend toward an increase at  $\text{Re} = 600$ , when compared directly to biomass increases in unstirred RDB vessels from the same replicate experiment (Figure 6). The distribution of these ratios was also found to be statistically normal when compared to a Gaussian distribution using the Kalmogorov-Smirnov test. The discoid plaque morphology of EL-4 cells grown in RDB vessels under agitated conditions was observed at all of  $\text{Re}$  values, although overall there was no significant change in biomass increase per day of culture, either

with stirring at  $\text{Re} = 600$  ( $5.42 \pm 1.1$ - fold,  $n = 6$ ) or without stirring ( $5.30 \pm 1.1$ - fold,  $n = 6$ ), compared to flask cultures ( $6.11 \pm 0.94$ - fold,  $n = 6$ ) (Figure 7).

### 3.2. Metabolic and immunological observations of EL-4 bioreactor cultures

Cultures in RDB vessels were usually accompanied by a more notable acidification of the medium, as suggested by a more pronounced yellowing of the culture solution phenol red indicator in comparison to flask cultures. This acidification was a consequence of significantly higher proportions of lactate produced by EL-4 cells relative to glucose consumption, in stirred RDB vessels ( $1.283 \pm 0.09$ ,  $n = 4$ ) compared to flask cultures ( $0.935 \pm 0.04$ ,  $n = 4$ ,  $p < 0.05$ ), with no differences observed between stirred and unstirred ( $1.281 \pm 0.10$ ) RDB cultures (Figure 8). Culture of EL-4 cells in RDB vessels was also accompanied by significant increase in the production of IL-4, either with stirring ( $938 \pm 81$  SFU,  $p < 0.05$ ) or without stirring ( $1114 \pm 138$  SFU  $p < 0.01$ ), compared to flask controls ( $386 \pm 16$  SFU) (Figure 9).

### 3.3. Effects of physicochemical conditions in bioreactors on EL-4 colony phenotype

The plaque phenotype of EL-4 cells aggregates cultured in bioreactors is suggestive of increased adhesion to the plastic substrate. Considering that this adherent phenotype was observed under both stirred and unstirred culture conditions, it is most likely that the phenotypic transformation was related to the potentially hypoxic environment. One reason for oxygen deprivation is its potentially limited diffusion to basally located cells, due to a relatively large fluid height (35–40 mm) compared to tissue culture flasks (5–10 mm), as well as differences in fluid surface area. It has been shown theoretically that oxygen transport efficiency in stirred RDBs can be trebled by simply halving the fluid level despite mixing at values greater than  $\text{Re} = 1200$  [18]. Initial testing of free standing, open RDB vessels with EL-4 cultures using similar levels of culture solution used in tissue culture flasks resulted in spheroid morphologies, as opposed to adherent plaques (results not shown). A fluid height aspect approximately equal to the diameter of RDB vessels was however maintained for the present study, since atmospheric oxygen was used during culture and hypoxic conditions (of the order of less than 5%) are more akin to the physiologically relevant values occurring within normal living tissues and solid tumors. Therefore, RDB vessels of these aspect ratios may represent a normoxic and potentially protective environmental against oxidative stresses (discussed in [29]).

In support of responses to a hypoxic environment is the observed increase in the conversion of glucose to lactate by EL-4 cells under stirred and unstirred bioreactor conditions, indicating increased anaerobic respiration. This is reminiscent of the so-called “Warburg effect” [30], a hallmark of cancer cells types due to abnormalities in aerobic glycolysis that cause inefficient oxygen metabolism, increased anaerobic glucose-to-lactate conversion, and increased sensitivity

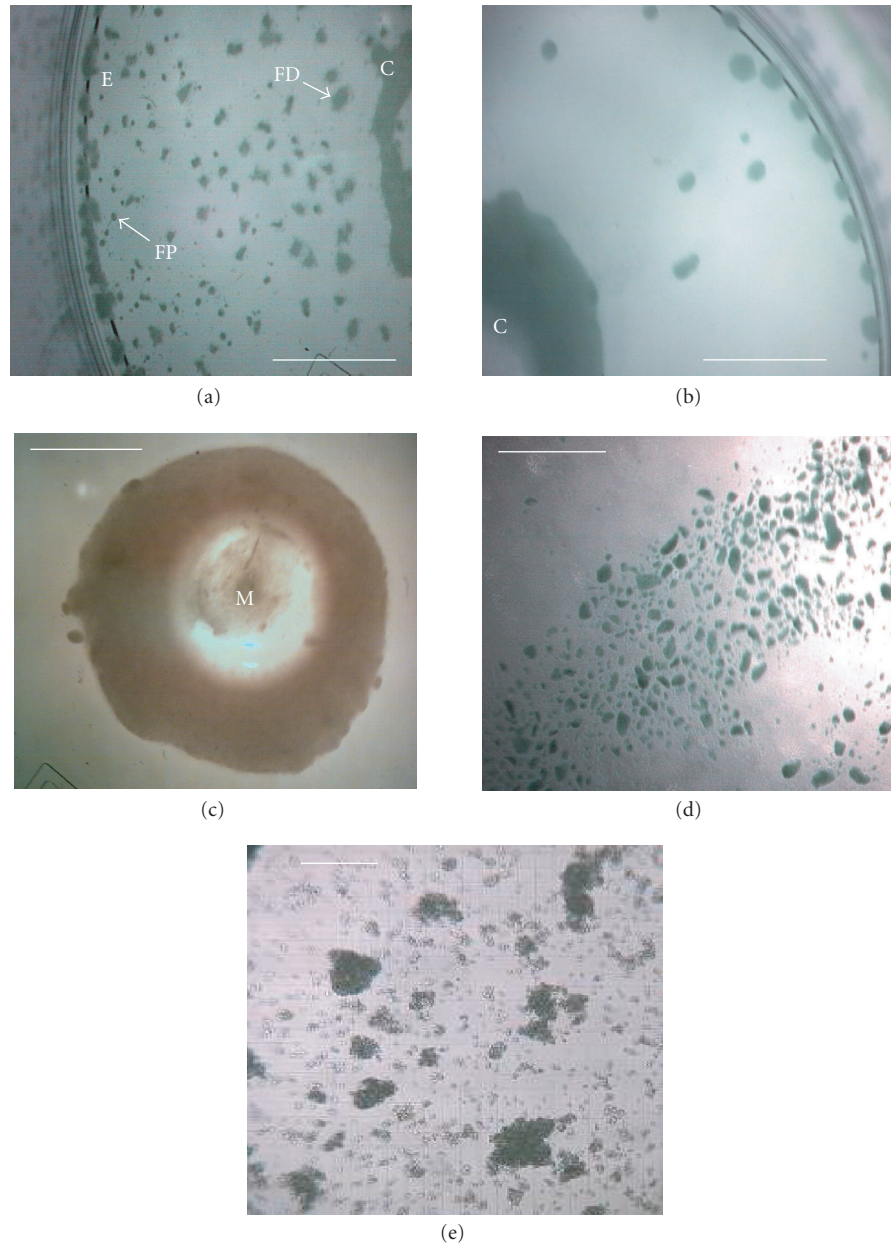


FIGURE 5: *Micrographs of bioreactor cultures.* (a) Base of a sector of an RDB bioreactor vessel following culture of EL-4 cells (without impeller agitation). EL-4 cells are dispersed across the surface as irregularly shaped plaques, with plaques merging into more confluent, continuous layers centrally (C) and along the circumferential edge (E), near the vessel side-wall. Intervening plaques located closer to the sidewall appear more focal punctate (FP) compared to more centrally located flattened discoid plaques (FD). (b) Base of a bioreactor vessel following culture of EL-4 cells with impeller agitation. Adherent plaques are larger discoid plaques, predominantly located centrally (C) and circumferentially (E), with a larger confluent tumor-like plaque with similarly smooth and flattened discoid appearance. (c) Magnified image of the central aggregate or “tumor” appearing in (b) showing a discoid, opaque colony with smooth edges. The centre of the plaque appears transparent due to a central dimple (manufacturing artefact) located on the plastic surface, a manufacturing artefact of the vessel over which a type of attenuated monolayer is visible (M). (d) Image of EL-4 aggregates of variable size, as viewed within a static tissue culture flasks. (e) Magnified image of EL-4 spheroid aggregates and disaggregated single cells contained on a hemocytometer slide, showing that spheroids are comprised of a homogeneous colony of densely packed, adherent cells. Scale bar = 10 mm (a)–(d) and 0.25 mm (e).

to aerobic conditions (reviewed in [31, 32]). Of particular importance is a recent report of the up-regulated expression of genes coding for a range of cell-substrate adhesion molecules in human colon cancer cells grown *in vitro* under

hypoxic conditions [33]. Taken together with more generic evidence, including associations between tumor adhesiveness and (reviewed in [34]) the ability of hypoxia to promote tumor progression and angiogenesis [35, 36], it is plausible

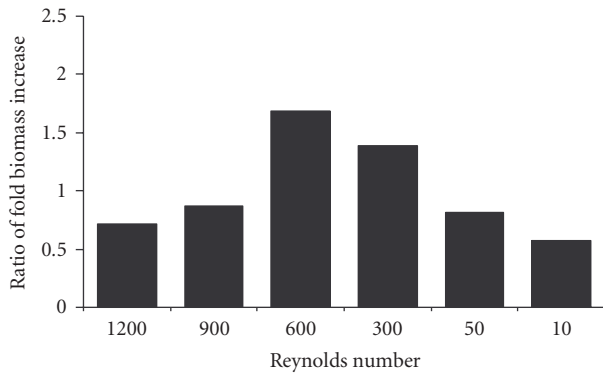


FIGURE 6: *Effect of stirring rate on cell growth in bioreactors.* Graph of the biomass increase of EL-4 cell colonies after culture in stirred rotating bioreactors at a range of rotational speeds, compared to no rotation.

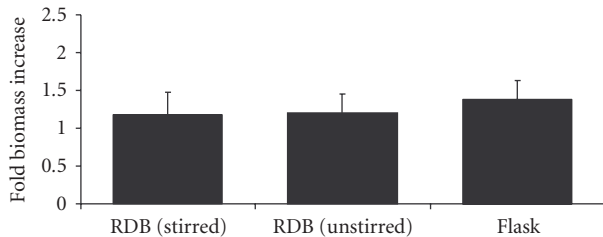


FIGURE 7: *Cell growth in bioreactors versus standard vessels.* Graph of biomass increase in EL-4 colonies after culture in rotating disc bioreactors with stirring ( $Re = 600$ ) or without stirring, compared to values of static flask cultures. Bars represent a mean of 6 experimental groups; error bars represent standard error of that mean.

that the plaque morphology represents an invasive phenotype. The observation of significantly increased antigenicity of EL-4 cells in RDB cultures for IL-4 known to be among a group of over-expressed cytokine markers of malignant lymphomas (reviewed in [37]) further establishes the plaques as an invasive phenotype. Further investigations, such as culture of EL-4 plaque-derived cells in three dimensional adhesion cultures [1], or following small animal inoculation may shed further light on this notion.

The variations in morphology of EL-4 plaques in stirred RDB vessels compared to those grown in static RDB vessels suggest a more distinct biological response to local mechanical stimulation. The potentially marginal improvement in EL-4 cell biomass increase indicated at  $Re$  values of around 600 confirms a potential shear-sensitivity of these cells as observed previously for cancer cell lines in other bioreactor types [6, 38], although the RDB vessels have far lower maximal and local shear distributions [17], which are further ameliorated by the use of serum in the culture solution [39]. Interestingly, the accumulation of a majority of EL-4 cells in a central aggregate occurred in a region of low-shear stress [16, 17] and high oxygenation [18]. While these regions may therefore be relatively less cytotoxic, accumulation of plaques here is more likely to represent a physical response of the spheroids to the fluid flow characteristics,

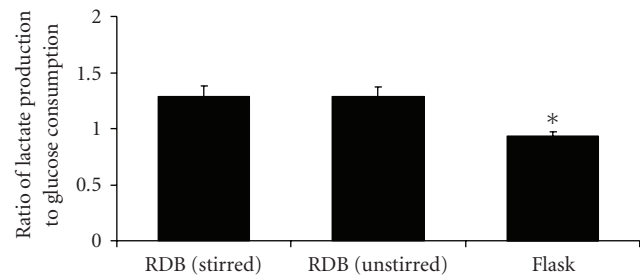


FIGURE 8: *Lactate production in bioreactor cultures.* Graph of lactate production by EL-4 colonies after culture in rotating disc bioreactors with stirring ( $Re = 600$ ) or without stirring, compared to values of static flask cultures. Bars represent the means of 3 experimental groups; error bars represent standard error of the mean; the asterisk pertains to  $P < .05$ .

causing centrifugation of entrapped aggregates [40] as predicted by the computational simulations (Figure 3(a)). For instance, plaques were notably absent from the intervening surface between the centre and the circumference of the vessel base, which corresponds to the highest regions of average shear stress at this boundary (Figure 4). Also, circumferentially located plaques are likely to have formed from aggregates entrapped in the simulated corner eddy evident at lower Reynolds numbers (Figure 3(a)). Furthermore, the apparently streamlined profile of these smaller discoid plaques suggests a response to gradual meridional shearing, which is also reflected in the streamlined and sharply edged central masses of EL-4 cells located centrally. Overall, these biomechanical stimuli are likely to influence how and where smaller aggregates coalesce to form larger ones, as indicated by the lower number of discoid plaques occupying a relatively larger surface area.

In biological terms, the morphology of the discoid plaques grown under stirred conditions could be regarded as similar to types of spherical metastatic lymphoma nodules observed in solid tissues observed in vivo, such as in the kidney and liver following EL-4 cell inoculation and lodgement within discrete tissue micro-environments [41]. In such cases, physical entrapment of cells may inevitably promote focal adhesions, resulting in increased rates of expansion of the lymphomas in situ. The precise biological consequences of the discoid plaque morphology remains to be determined, however a potential amelioration of IL-4 secretion by EL-4 cells in stirred RDBs rather than unstirred RDBs (Figure 9) warrants further investigation, especially in light of reported modulations of cytokine secretion by hybridomas under modified hydrodynamic conditions [23, 42].

### 3.4. Future prospects for bioreactors as a research tool for cancer biology

The rotating disc bioreactor appears to be comparable to standard culture vessels for supporting the propagation of a cancer cell type in vitro. This study also demonstrates the feasibility of directly adapting generic biotechnologies to research applications with downstream applications to

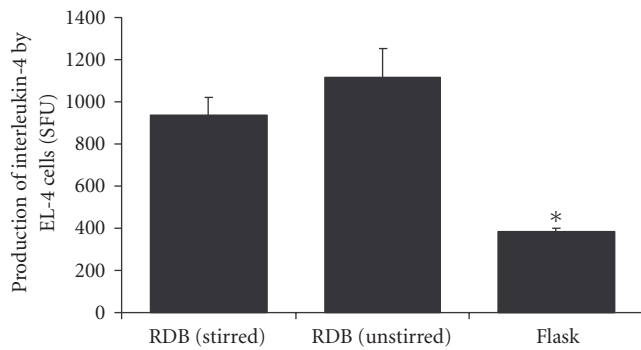


FIGURE 9: Cytokine production in bioreactor cultures. Graph of interleukin-4 production by EL-4 colonies after culture in rotating disc bioreactors with stirring ( $Re = 600$ ) or without, compared to values of static flask cultures. Bars represent the means of 3 experimental groups; error bars represent standard error of the mean; the asterisk pertains to  $P < .05$ .

biomedical sciences. The versatility of bioreactor approaches is illustrated in a number of relevant applications, including isolation of rare forms of cancer stem cells [10], assessment of cancer pharmacological strategies [9] and for systematic regeneration of a range of solid tissue types as replacements for those damaged or surgically removed as a consequence of cancer (reviewed in [43]). While the described RDB design probably requires further refinement for mammalian cell culture (e.g., optimization of fluid heights, impeller location, stirring frequency, inclusion of perfused solutions, automation of control, and environmental sensing) this simple, scalable, and economical form of stirred culture bioreactor could be amenable to a variety of research applications in cancer biology. In addition to modelling the effects of hypoxia, possibilities include establishment of more effective three-dimensional tumor constructs, modeling of long-term tumor progression, alternative large-scale generation of hybridomas for tumor antibody production, and development of improved multicellular spheroid cocultures for angiogenesis models [44].

## ACKNOWLEDGMENTS

The authors wish to sincerely thank the technical staff at Monash University Department of Mechanical Engineering Workshop for construction of the bioreactor rig; Professor Richard Boyd at Monash Immunology and Stem Cell Laboratories (MISCL) and his colleagues Dr. Anne Chidgey and Mr Mark Malin for providing starter cultures of EL-4 cells; Dr. Tayfur Tecirlioglu (MISCL) for loan of a hemocytometer; Ms Julie Newman and Mr Michael Daskalakis at Monash Medical Centre Biochemistry Department for their assistance in performing glucose and lactate assays; Professor Duk At Nguyen (Rheology lab, Monash University Department of Chemical Engineering) for his assistance in performing viscosity measurements of culture solutions, Dr. Wan Shoo Cheong at the Monash University Department of Microbiology for her assistance in performing ELISPOT assays, Dr. Andreas Fouras and Dr. David Lo Jacono of the

Division of Biological Engineering for their assistance with fluid mechanical aspects. Finally, the authors wish to thank Associate Professor Mark Thompson for his valuable assistance in simulation of flow characteristics. This research was supported by Australian Research Council (ARC) Discovery Grant DP0452664.

## REFERENCES

- [1] M. M. Mareel, "Invasion in vitro-methods of analysis," *Cancer And Metastasis Review*, vol. 2, no. 2, pp. 201–218, 1983.
- [2] R. Auerbach, R. Lewis, B. Shinnars, L. Kubai, and N. Akhtar, "Angiogenesis assays: a critical overview," *Clinical Chemistry*, vol. 49, no. 1, pp. 32–40, 2003.
- [3] D. M. Pirone and C. S. Chen, "Strategies for engineering the adhesive microenvironment," *Journal of Mammary Gland Biology and Neoplasia*, vol. 9, no. 4, pp. 405–417, 2004.
- [4] Y. Martin and P. Vermette, "Bioreactors for tissue mass culture: design, characterization, and recent advances," *Biomaterials*, vol. 26, no. 35, pp. 7481–7503, 2005.
- [5] R. P. Schwarz, T. J. Goodwin, and D. A. Wolf, "Cell culture for three-dimensional modeling in rotating-wall vessels: an application of simulated microgravity," *Journal of Tissue Culture Methods*, vol. 14, no. 2, pp. 51–57, 1992.
- [6] S. J. Curran and R. A. Black, "Oxygen transport and cell viability in an annular flow bioreactor: comparison of laminar Couette and Taylor-vortex flow regimes," *Biotechnology and Bioengineering*, vol. 89, no. 7, pp. 766–774, 2005.
- [7] W. M. Miller, H. W. Blanch, and C. R. Wilke, "Kinetic analysis of hybridoma growth and metabolism in batch and continuous suspension culture: effect of nutrient concentration, dilution rate, and pH," *Biotechnology and Bioengineering*, vol. 67, no. 6, pp. 853–871, 2000.
- [8] M. Ingram, G. B. Techy, R. Saroufeem, et al., "Three-dimensional growth patterns of various human tumor cell lines in simulated microgravity of a NASA bioreactor," *In Vitro Cellular & Developmental Biology*, vol. 33, no. 6, pp. 459–466, 1997.
- [9] M. N. Kirstein, R. C. Brundage, W. F. Elmquist, et al., "Characterization of an in vitro cell culture bioreactor system to evaluate anti-neoplastic drug regimens," *Breast Cancer Research and Treatment*, vol. 96, no. 3, pp. 217–225, 2006.
- [10] B. S. Youn, A. Sen, L. A. Behie, A. Girgis-Gabardo, and J. A. Hassell, "Scale-up of breast cancer stem cell aggregate cultures to suspension bioreactors," *Biotechnology Progress*, vol. 22, no. 3, pp. 801–810, 2006.
- [11] T. Hongo, M. Kajikawa, S. Ishida, et al., "Gene expression property of high-density three-dimensional tissue of HepG2 cells formed in radial-flow bioreactor," *Journal of Bioscience and Bioengineering*, vol. 101, no. 3, pp. 243–250, 2006.
- [12] L. E. Freed and G. Vunjak-Novakovic, "Microgravity tissue engineering," *In Vitro Cellular & Developmental Biology*, vol. 33, no. 5, pp. 381–385, 1997.
- [13] I. Mérida and A. Avila-Flores, "Tumor metabolism: new opportunities for cancer therapy," *Clinical & Translational Oncology*, vol. 8, no. 10, pp. 711–716, 2006.
- [14] J. M. Cuezva, M. Krajewska, M. L. de Heredia, et al., "The bioenergetic signature of cancer: a marker of tumor progression," *Cancer Research*, vol. 62, no. 22, pp. 6674–6681, 2002.
- [15] R. B. Herberman, "Serological analysis of cell surface antigens of tumors induced by murine leukemia virus," *Journal of the National Cancer Institute*, vol. 48, no. 1, pp. 265–271, 1972.



- [16] M. P. Escudier, "Observations of the flow produced in a cylindrical container by a rotating endwall," *Experiments in Fluids*, vol. 2, no. 4, pp. 189–196, 1984.
- [17] J. Dusting, J. Sheridan, and K. Hourigan, "A fluid dynamics approach to bioreactor design for cell and tissue culture," *Biotechnology and Bioengineering*, vol. 94, no. 6, pp. 1196–1208, 2006.
- [18] P. Yu, T. S. Lee, Y. Zeng, and H. T. Low, "Effect of vortex breakdown on mass transfer in a cell culture bioreactor," *Modern Physics Letters B*, vol. 19, no. 28-29, pp. 1543–1546, 2005.
- [19] L. Mununga, M. C. Thompson, and K. Hourigan, "Comparative study of flow in a mixing vessel stirred by a solid disk and a four bladed impeller," in *Proceedings of the 14th Australasian Fluid Mechanics Conference*, pp. 661–664, Adelaide, Australia, December 2001.
- [20] D. Lo Jacono, K. Hourigan, and J. Sorensen, "Vortex breakdown in a closed cylinder: experiments and control," in *Proceedings of the 59th Annual Meeting of the Division of Fluid Dynamics*, vol. 51, p. 119, Tampa Bay, Fla, USA, November 2006.
- [21] W. R. Benjamin and J. J. Farrar, "Biological and biochemical properties of lymphokines produced by the EL 4 thymoma cell line," *Lymphokine Research*, vol. 2, no. 1, pp. 33–36, 1983.
- [22] J. W. Schrader, B. A. Cunningham, and G. M. Edelman, "Functional interactions of viral and histocompatibility antigens at tumor cell surfaces," *Proceedings of the National Academy of Sciences of the United States of America*, vol. 72, no. 12, pp. 5066–5070, 1975.
- [23] L. Richert, A. Or, and M. Shinitzky, "Promotion of tumor antigenicity in EL-4 leukemia cells by hydrostatic pressure," *Cancer Immunology, Immunotherapy*, vol. 22, no. 2, pp. 119–124, 1986.
- [24] M. Malin, "Basic Tissue Culture Techniques," <http://users.monash.edu.au/~malin/methods.htm>, 2005.
- [25] M. Stettler, N. Jaccard, D. Hacker, M. de Jesus, F. M. Wurm, and M. Jordan, "New disposable tubes for rapid and precise biomass assessment for suspension cultures of mammalian cells," *Biotechnology and Bioengineering*, vol. 95, no. 6, pp. 1228–1233, 2006.
- [26] F. L. Moolten and B. Schreiber, "Formation of adherent monolayers of murine lymphocytes in vitro: the use of serum-free medium and concanavalin A-coated surfaces to promote adherence," *Journal of Immunological Methods*, vol. 36, no. 3-4, pp. 359–368, 1980.
- [27] S. S. Ozturk and B. O. Palsson, "Effect of initial cell density on hybridoma growth, metabolism, and monoclonal antibody production," *Journal of Biotechnology*, vol. 16, no. 3-4, pp. 259–278, 1990.
- [28] W. S. Hu, T. C. Dodge, K. K. Frame, and V. B. Himes, "Effect of glucose on the cultivation of mammalian cells," *Developments in Biological Standardization*, vol. 66, pp. 279–290, 1987.
- [29] E. Gnaiger, "Bioenergetics at low oxygen: dependence of respiration and phosphorylation on oxygen and adenosine diphosphate supply," *Respiration Physiology*, vol. 128, no. 3, pp. 277–297, 2001.
- [30] O. Warburg, "The reaction of ascites tumor cells to oxygen under high pressure," *Archiv für Geschwulstforschung*, vol. 6, no. 1, pp. 7–11, 1953.
- [31] J.-W. Kim and C. V. Dang, "Cancer's molecular sweet tooth and the warburg effect," *Cancer Research*, vol. 66, no. 18, pp. 8927–8930, 2006.
- [32] H. Pelicano, D. S. Martin, R.-H. Xu, and P. Huang, "Glycolysis inhibition for anticancer treatment," *Oncogene*, vol. 25, no. 34, pp. 4633–4646, 2006.
- [33] T. Koike, N. Kimura, K. Miyazaki, et al., "Hypoxia induces adhesion molecules on cancer cells: a missing link between Warburg effect and induction of selectin-ligand carbohydrates," *Proceedings of the National Academy of Sciences of the United States of America*, vol. 101, no. 21, pp. 8132–8137, 2004.
- [34] R. A. Cairns, R. Khokha, and R. P. Hill, "Molecular mechanisms of tumor invasion and metastasis: an integrated view," *Current Molecular Medicine*, vol. 3, no. 7, pp. 659–671, 2003.
- [35] C. Z. Michaylira and H. Nakagawa, "Hypoxic microenvironment as a cradle for melanoma development and progression," *Cancer Biology and Therapy*, vol. 5, no. 5, pp. 476–479, 2006.
- [36] L. Chen and F. Shibasaki, "Angiogenesis and metastasis of carcinoma," *Clinical Calcium*, vol. 16, no. 4, pp. 613–619, 2006.
- [37] S.-M. Hsu, J. W. Waldron Jr., P.-L. Hsu, and A. J. Hough Jr., "Cytokines in malignant lymphomas: review and prospective evaluation," *Human Pathology*, vol. 24, no. 10, pp. 1040–1057, 1993.
- [38] J. F. Petersen, L. V. McIntire, and E. T. Papoutsakis, "Shear sensitivity of hybridoma cells in batch, fed-batch, and continuous cultures," *Biotechnology Progress*, vol. 6, no. 2, pp. 114–120, 1990.
- [39] S. S. Ozturk and B. O. Palsson, "Examination of serum and bovine serum albumin as shear protective agents in agitated cultures of hybridoma cells," *Journal of Biotechnology*, vol. 18, no. 1-2, pp. 13–28, 1991.
- [40] J. Lee and A. J. C. Ladd, "Axial segregation in a cylindrical centrifuge," *Physical Review Letters*, vol. 89, no. 10, Article ID 104301, 1–4, 2002.
- [41] L. Ding, M. Sunamura, T. Kodama, et al., "In vivo evaluation of the early events associated with liver metastasis of circulating cancer cells," *British Journal of Cancer*, vol. 85, no. 3, pp. 431–438, 2001.
- [42] T. Ryll, M. Lucki-Lange, V. Jager, and R. Wagner, "Production of recombinant human interleukin-2 with BHK cells in a hollow fibre and a stirred tank reactor with protein-free medium," *Journal of Biotechnology*, vol. 14, no. 3-4, pp. 377–392, 1990.
- [43] J. F. Stoltz, D. Bensoussan, V. Decot, P. Netter, A. Ciree, and P. Gillet, "Cell and tissue engineering and clinical applications: an overview," *Bio-Medical Materials and Engineering*, vol. 16, supplement 4, pp. S3–S18, 2006.
- [44] A. Wenger, A. Stahl, H. Weber, et al., "Modulation of in vitro angiogenesis in a three-dimensional spheroidal coculture model for bone tissue engineering," *Tissue Engineering*, vol. 10, no. 9-10, pp. 1536–1547, 2004.